



ELSEVIER

Contents lists available at ScienceDirect

Redox Biology

journal homepage: www.elsevier.com/locate/redox

Research paper

Mitochondrial contribution to lipofuscin formation

Jeannette König^a, Christiane Ott^a, Martín Hugo^a, Tobias Jung^{a,d}, Anne-Laure Bulteau^b,
Tilman Grune^{a,c,d,e}, Annika Höhn^{a,c,*}

^a Department of Molecular Toxicology, German Institute of Human Nutrition Potsdam-Rehbruecke (DIfE), 14558 Nuthetal, Germany

^b Institut de Génétique Fonctionnelle de Lyon (IGFL) – ENS de Lyon, 69007 Lyon, France

^c German Center for Diabetes Research (DZD), 85764 München-Neuherberg, Germany

^d German Center for Cardiovascular Research (DZHK), 10117 Berlin, Germany

^e NutriAct-Competence Cluster Nutrition Research Berlin-Potsdam, Nuthetal 14458, Germany



ARTICLE INFO

Keywords:

Lipofuscin
Protein aggregates
Lon protease
Aging
Mitochondria
Oxidative stress

ABSTRACT

Mitochondria have been in the focus of oxidative stress and aging research for decades due to their permanent production of ROS during the oxidative phosphorylation. The hypothesis exists that mitochondria are involved in the formation of lipofuscin, an autofluorescent protein aggregate that accumulates progressively over time in lysosomes of post-mitotic and senescent cells. To investigate the influence and involvement of mitochondria in lipofuscinogenesis, we analyzed lipofuscin amounts as well as the mitochondrial function in young and senescent cells. In addition we used an aging model and Lon protease deficient HeLa cells to investigate the influence of mitochondrial degradation processes on lipofuscin formation.

We were able to show that mitophagy is impaired in senescent cells resulting in an increased mitochondrial mass and superoxide formation. In addition, the inhibition of mitochondrial fission leads to increased lipofuscin formation.

Moreover, we observed that Lon protease downregulation is linked to a higher lipofuscinogenesis whereas the application of the mitochondrial-targeted antioxidant mitoTEMPO is able to prevent the accumulation of this protein aggregate.

1. Introduction

The intracellular accumulation of protein aggregates is one important hallmark of the aging process [1]. Especially cells with a low mitotic rate accumulate high amounts of protein aggregation products during their lifetime [2–4]. In this context the formation of covalent cross-linked protein aggregates, such as lipofuscin, is of special importance because of its abundance in aged cells where it has detrimental effects. For instance, it is clearly established that lipofuscin is able to inhibit intracellular proteostasis mechanisms, especially proteasomal activity and, therefore, the effective degradation of

oxidatively modified proteins [3, 5–8]. This in turn leads to an increased formation of protein aggregation products further promoting the formation of lipofuscin [9]. Additionally, it was shown that lipofuscin generates reactive oxygen species (ROS) due to its ability to incorporate redox-active metals such as iron, thus promoting the Fenton reaction [10]. Moreover, the accumulation of lipofuscin is of pathophysiological relevance. In this regard, it was shown that an accelerated accumulation is linked to the development of neurological diseases such as Alzheimer's disease [11] and Parkinson's disease [12] as well as age-related macular degeneration, which seems to be the most frequent reason for blindness in the Western world [13].

Abbreviations: CCCP, Carbonyl cyanide 3-chlorophenylhydrazone; COX IV, Cytochrome c oxidase subunit IV; DAPI, 4',6-Diamidino-2-phenylindole dihydrochloride; DMEM, Dulbecco's Modified Eagle Medium; DMSO, Dimethyl sulfoxide; Drp-1, Dynamin-related protein 1; DNPH, 2,4-dinitrophenylhydrazine; DNP, 2,4-dinitrophenylhydrazine; Dox, Doxycycline; EDTA, Ethylenediaminetetraacetic acid; Em, Emission wavelength; ETC, Electron transport chain; Ex, Excitation wavelength; FBS, Fetal bovine serum; FCCP, Carbonyl cyanide 4-(trifluoromethoxy) phenylhydrazone; Fis1, Mitochondrial fission 1 protein; FITC, Fluorescein isothiocyanate; H₂DCFDA, 2',7'-Dichlorodihydrofluorescein diacetate; Ki-67, Kiel 67 protein; Mdivi-1, Mitochondrial division inhibitor 1; MitoTEMPO, (2-(2,2,6,6-Tetramethylpiperidin-1-oxyl-4-ylamino)-2-oxoethyl)triphenyl-phosphonium chloride; MT-CO1, mitochondrially encoded cytochrome c oxidase I; mtDNA, Mitochondrial DNA; MTG, MitoTracker Green^{FM}; MTT, Methylthiazolyl-diphenyl-tetrazolium bromide; OCR, Oxygen consumption rate; PI, propidium iodide; PINK1, PTEN-induced putative kinase 1; PQ, Paraquat; ROS, Reactive oxygen species; RNAi, RNA interference; SA-β-Gal, Senescence associated β-galactosidase; SDHA, Succinate Dehydrogenase Complex Flavoprotein Subunit A; shRNA, Short hairpin RNA; SIPS, Stress-induced premature senescence; SDS, Sodium dodecyl sulfate; VDAC, Voltage-dependent anion channel

* Correspondence to: German Institute of Human Nutrition Potsdam-Rehbruecke, Arthur-Scheunert-Allee 114-116, 14558 Nuthetal, Germany.

E-mail addresses: jeannette.koenig@dife.de (J. König), christiane.ott@dife.de (C. Ott), martin.hugo@dife.de (M. Hugo), tobias.jung@dife.de (T. Jung), anne-laure.bulteau@ens-lyon.fr (A.-L. Bulteau), scientific.director@dife.de (T. Grune), annika.hoehn@dife.de (A. Höhn).

<http://dx.doi.org/10.1016/j.redox.2017.01.017>

Received 17 January 2017; Accepted 23 January 2017

Available online 25 January 2017

2213-2317/© 2017 The Authors. Published by Elsevier B.V.

This is an open access article under the CC BY-NC-ND license (<http://creativecommons.org/licenses/by-nc-nd/4.0/>).

The cellular consequences of lipofuscin accumulation are well studied. However, no data are available on its protein sources from different protein pools such as cytosolic or organelle proteins in the formation of lipofuscin. Nevertheless, it can be hypothesized that the composition of lipofuscin is strongly dependent on the intracellular site of ROS attack and, therefore, different oxidatively modified proteins and lipids might contribute to the formation of lipofuscin. However, it is postulated that especially mitochondria are involved in the development of lipofuscin. The hypothesis of Terman and Brunk, referred to as the “mitochondrial-lysosomal axis theory of aging” assumes the incomplete degradation of damaged mitochondria mediated by autophagy as the cause for lipofuscin accumulation [14]. Although this hypothesis has not clearly been experimentally proven, some results found in the literature support this hypothesis.

This includes for example the finding of the mitochondrial ATP synthase subunit c as a major component in lipofuscin formed under pathological conditions during the progression of neuronal ceroid lipofuscinosis (NCL) [15]. Furthermore, it is generally accepted that mitochondria are the primary site of ROS formation in normal metabolism [16,17]. Moreover, it was shown that mitochondrial DNA mutations which accumulate during aging lead to further mitochondrial malfunction [18,19], and that the mitochondrial protease Lon which is able to degrade oxidatively modified mitochondrial proteins declines during aging [20–22]. Also these findings strengthen the hypothesis of a potential mitochondrial involvement in lipofuscin formation.

The system to remove damaged mitochondria effectively is generally believed to be mitophagy [23,24]. Recently we were able to demonstrate a reduction of macroautophagic processes in senescent cells and murine brain tissue [25,26]. Before mitophagy occurs, the mitochondrial network frequently undergoes fusion and fission processes, as a part of the mitochondrial quality control and to ensure mitochondrial integrity [27]. Interestingly, fission occurs mainly as the initial step of mitochondria-selective autophagy and ensures, thereby, the adequate degradation of damaged or dysfunctional mitochondria by the lysosomal system [28].

The aim of this study was to investigate the role of mitochondrial proteins and mitochondrial protein oxidation on lipofuscinogenesis; especially to reveal whether mitophagy or the Lon protease are effective in the protecting of cells from lipofuscin formation.

2. Materials and methods

2.1. Materials

Chemicals were purchased from Sigma-Aldrich (Deisenhofen, Germany) except Mdivi-1 (Enzo Life Science, Lörrach, Germany) as well as doxycycline, blasticidin and zeocin (Invivogen, San Diego, CA, USA). Cell culture materials and media were obtained from Biochrom (Berlin, Germany). MitoTracker Green^{FM} (MTG) and MitoSOXTM Red superoxide indicator (MitoSOX) were purchased from Molecular Probes (Eugene, USA).

The following primary antibodies were used: rabbit anti-DNP (Sigma-Aldrich, Deisenhofen, Germany), rabbit anti-PINK1 (Cell Signaling, Boston, MA, USA), mouse anti- β -actin (Cell Signaling, Boston, USA), rabbit anti-COX IV (Cell Signaling, Boston, MA, USA), rabbit anti-Lon protease (Abcam, Cambridge, UK), mouse anti-GAPDH (Abcam, Cambridge, UK), rabbit anti-Ki-67 (Abcam, Cambridge, UK), mouse anti-CDKN2A/p16INK4a (Abcam, Cambridge, UK), rabbit anti-p21 Waf1/Cip1 (Cell Signaling, Boston, MA, USA), mouse anti-MT-CO1 (Abcam, Cambridge, UK), mouse anti-SDHA (Abcam, Cambridge, UK), mouse anti-VDAC (Abcam, Cambridge, UK) and rabbit anti-Fis1 (Cell Signaling, Boston, MA, USA). Secondary antibodies used for immunoblotting were purchased from LI-COR Biosciences (Lincoln, AL, USA). The FITC-labeled antibody for immunofluorescence was purchased from Invitrogen (Carlsbad, CA, USA).

2.2. Cell culture

Experiments were performed by using primary human dermal fibroblasts as well as Lon protease deficient HeLa cells. Human dermal fibroblasts were divided in two categories: “young” and “senescent”. Young fibroblasts were obtained from human skin tissue of a 1-year old donor, kindly provided by Prof. Scharffetter-Kochanek (University of Ulm, Germany). Senescent fibroblasts originated from human skin tissue of a 81-year old donor and were kindly provided by Beiersdorf AG (Hamburg, Germany) [29]. Fibroblasts were grown in high-glucose (4.5 g/l) Dulbecco's Modified Eagle's Medium (DMEM) with 5% glutamine and 10% fetal bovine serum (FBS) at 7% CO₂, 95% humidity and 37 °C.

Lon protease deficient HeLa cells were kindly provided by Dr. Anne-Laure Bulteau (Institute of Functional Genomics of Lyon, France). Experimental design and establishment of these cells was described previously [30,31]. In brief, Lon protease deficient HeLa cells were generated using HeLa T-RexTM cells (Invitrogen Life Technology, Carlsbad, CA, USA) which were stably transfected with the short hairpin RNA (shRNA) expressing vector pENTR/H1/T0+(Invitrogen, BLOCK-ITTM). For the realization of Lon protease knockdown a Lon-specific 68-base sequence complementary oligonucleotide was cloned into the pENTR/H1/T0+ vector. Furthermore, the expression of the Lon-specific shRNA underlies a doxycycline (Dox)-regulated promoter (tet-on system). Therefore, the addition of Dox to the medium resulted in the expression of shRNA against Lon protease leading subsequently to the downregulation of this enzyme. Clones of HeLa-tet-on-shLon cells were selected in low-glucose (1 g/l) DMEM with 10% FBS, 5% glutamine, 5 μ g/ml blasticidin and 200 μ g/ml zeocin. Cultivation was carried out at 7% CO₂, 95% humidity at 37 °C. Expression of Lon-specific shRNA was induced by the addition of 2 μ g/ml doxycycline to the medium for 10 days. During this period medium was replaced every second day with fresh Dox. Efficacy of Lon protease knockdown was verified by immunoblotting.

2.3. Stress-induced premature senescence (SIPS)

For the induction of intracellular lipofuscin formation cells were chronically treated with paraquat (PQ) for 10 days. This procedure is known as stress-induced premature senescence (SIPS) and is described elsewhere in detail [32]. To induce premature senescence in fibroblasts, confluent cells were incubated daily with 40 μ M PQ for a period of 10 days. In contrast to fibroblasts, HeLa Lon cells were treated in a subconfluent state with 20 μ M PQ for 10 days. SIPS of HeLa Lon cells started after the ten-day Dox treatment for initial Lon protease downregulation. However, Lon protease downregulation was also continued during SIPS by adding Dox to the medium. Mdivi-1 (mitochondrial division inhibitor-1) as well as mitoTEMPO was applied by co-incubation with PQ. Fibroblasts received 50 μ M Mdivi-1 or 2.5 μ M mitoTEMPO. HeLa Lon cells were treated with 5 μ M Mdivi-1 or 10 μ M mitoTEMPO.

2.4. Senescence-associated β -galactosidase staining

β -Galactosidase activity was determined at pH 6 using “Senescence-associated β -galactosidase staining Kit” from Cell Signaling (Boston, USA) according to manufacturer's instructions.

2.5. Lipofuscin detection

Detection and quantification of lipofuscin was performed by measurement of its autofluorescence [33] either by confocal microscopy (Laser scanning microscope 700, Carl Zeiss, Jena, Germany) (Ex: 405 nm; Em: 498 nm) or by flow cytometry with the Cell Lab QuantaTM SC MPL (Beckman Coulter GmbH, Krefeld, Germany) or the MACSQuant[®] Analyzer 10; (Miltenyi Biotec, Bergisch Gladbach,

Germany).

2.6. Measurement of oxygen consumption rates (OCRs)

For the assessment of mitochondrial function of young and senescent fibroblasts, oxygen consumption rates were analyzed after manipulating specific targets of the electron transport chain (ETC) using an XF-24-3 extracellular flux analyzer (Seahorse Bioscience, North Billerica, USA). The analyzer detects changes in oxygen and proton concentrations in the medium surrounding the cells, allowing the simultaneous measurement of the cellular oxidation rate as well as the glycolytic metabolism. Cells were seeded one day before the assay onto XF-24 well culture plates (Seahorse Bioscience) in DMEM. On the next day, one hour prior the assay, cells were incubated in a DMEM-based medium with 1 mM pyruvate, 2 mM glutamine, and 10 mM glucose in a CO₂-free incubator. After basal OCRs were assessed, OCR responses after the successive application of oligomycin (1 μM), carbonyl cyanide 4-(trifluoromethoxy) phenylhydrazone (FCCP; 2 μM), and the mix of antimycin A (0.5 μM) and rotenone (0.5 μM) (XF Cell Mito Stress Kit, Seahorse Bioscience) were determined. OCRs were subsequently normalized to the protein concentration.

2.7. Detection of mitophagy

For the detection of mitophagy in young and senescent fibroblasts a novel Mitophagy Detection Kit (Dojindo Molecular Technologies, Rockville, USA) was used. Cells were treated according to the manufacturer's recommendations. In brief, cells were washed twice with DMEM and afterwards incubated at 37 °C for 30 min with 100 nmol Mtpgagy Dye diluted in DMEM. After this incubation cells were again washed twice with DMEM followed by the addition of complete DMEM. The induction of mitophagy was then accomplished by the addition of 20 μM carbonyl cyanide 3-chlorophenylhydrazone (CCCP) for 24 h. Subsequently, fibroblasts were trypsinized and fluorescence intensity of Mtpgagy Dye was measured by flow cytometry at 488 nm excitation and 655–730 nm emission (MACSQuant® Analyzer 10; Miltenyi Biotec, Bergisch Gladbach, Germany). Thus, an increase in Mtpgagy Dye specific fluorescence intensity indicated the occurrence of mitophagy.

2.8. Determination of mitochondrial mass and mitochondrial superoxide

Fibroblasts were incubated with 500 nM MitoTracker Green^{FM} or 2.5 μM MitoSOXTM Red superoxide indicator for 30 min in complete medium for the analysis of mitochondrial mass and mitochondrial superoxide, respectively. Afterwards cells were washed with PBS, trypsinized and analyzed by flow cytometry either at Cell Lab QuantaTM SC MPL (Beckman Coulter GmbH, Krefeld, Germany) or MACSQuant® Analyzer 10; (Miltenyi Biotec, Bergisch Gladbach, Germany).

2.9. Cellular ROS levels

Intracellular ROS formation was measured via H₂DCFDA-assay. Cells were loaded with 5 μM cell-permeable H₂DCFDA for 1 h. Intracellular oxidation of H₂DCFDA by ROS leads to its conversion into the highly fluorescent 2',7'-dichlorofluorescein (DCF). DCF fluorescence was estimated by flow cytometry using Cell Lab QuantaTM SC MPL (Beckman Coulter GmbH, Krefeld, Germany) after excitation at 488 nm and emission at 525 nm.

2.10. Cell viability assay

Viability of cells was measured by propidium iodide (PI) staining using PI at a final concentration of 1 μg/ml. PI was added to the cells

directly before each sample measurement. Specific PI fluorescence was measured by flow cytometry with a MACSQuant® Analyzer 10; (Miltenyi Biotec, Bergisch Gladbach, Germany).

2.11. Immunoblot

Cells were washed with PBS and subsequently scraped in SDS lysis buffer (10 mM Tris-HCl pH 7.5, 0.9% NP-40, 0.1% SDS, 1 mM pefablock) containing freshly added protease inhibitor cocktail (1:100) followed by a 30 min incubation time on ice. Afterwards, lysate protein concentrations were determined by DCTM Protein Assay (Bio-Rad GmbH, Munich, Germany) [34]. The amount of 15 μg protein was added to a reducing loading buffer (0.25 M Tris (pH 6.8), 8% SDS, 40% glycerol, 0.03% Orange G) followed by the denaturation of proteins at 95 °C for 5 min. For protein separation, 10 or 12% (w/v) SDS polyacrylamide gels were used. After gelelectrophoresis proteins were transferred onto nitrocellulose membrane (Whatman®, GE Healthcare, Dassel, Germany) by semi-dry blotting. Subsequently, membranes were blocked in Odyssey® blocking buffer (LI-COR Biosciences, Lincoln, USA) diluted in PBS (1:5) for 1 h at room temperature. Primary antibodies were diluted in Odyssey® blocking buffer according to supplier's suggestions and incubated over night at 4 °C. Fluorescence-coupled secondary antibodies were used for the detection of the proteins of interest. Blots were scanned and analyzed using an Odyssey® Infrared Imaging System (LI-COR Biosciences, Lincoln, NE, USA).

2.12. Detection of carbonylated proteins by immunoblot

Protein carbonyls are a common biomarker for oxidatively modified proteins [35]. Their detection was carried out by immunoblotting after derivatizing the carbonyl groups of the blotted proteins with 2,4-dinitrophenylhydrazine (DNPH). This reaction leads to the formation of a stable 2,4-dinitrophenylhydrazone (DNP) [36] which can be detected by an anti-DNP antibody.

2.13. Determination of the mitochondrial network size and Ki-67 staining

To estimate the size of the mitochondrial network in young and senescent fibroblasts, mitochondria were visualized by immunofluorescence staining followed by the quantification of the mitochondrial pixel area with Adobe Photoshop CC2014 (Adobe Systems Incorporated, San Jose, CA, USA). For immunostaining, cells were seeded on glass bottom dishes (MatTek Corporation, Ashland, USA) 24 h before the staining procedure. Then cells were washed with PBS and fixed with a mixture of ethanol: diethylether (1:1) for 5 min at –20 °C. Subsequently, cells were washed several times with PBS containing 1% FBS followed by blocking for 1 h at room temperature in the same buffer. Afterwards, fixed cells were incubated with an anti-COX IV antibody for mitochondrial staining or an anti-Ki-67 antibody over night at 4 °C. Antibodies were diluted in PBS containing 1% FBS 1:50 (anti-COX IV) and 1:250 (anti-Ki-67), respectively. This step was followed by the incubation with a secondary FITC-labeled antibody (diluted 1:500 in PBS/1% FBS) for 1 h at room temperature. For additional DNA staining cells were incubated with DAPI (1 μg/ml) for 10 min at room temperature. Microscopy was carried out using a laser scanning microscope (Carl Zeiss, Jena, Germany).

2.14. Statistical analysis

Statistical analysis was performed using Prism 6 (GraphPad, La Jolla, CA, USA) software. All results presented in the figures are mean values ± SD of at least 3 experiments. Differences between two groups were assessed by Student's *t*-test. Multiple comparisons were assessed either by one-way ANOVA followed by Tukey's post-hoc test or by two-

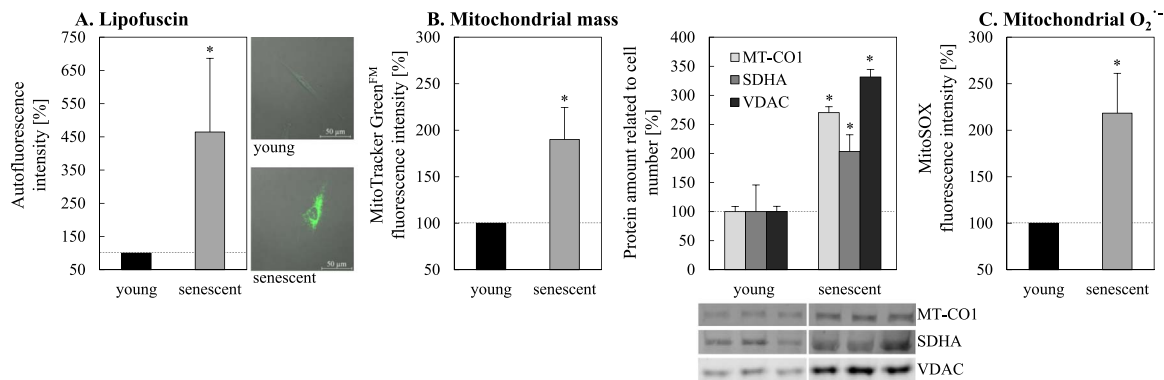


Fig. 1. Quantification of lipofuscin, mitochondria and mitochondrial superoxide production in young and senescent fibroblasts. Panel A shows the intracellular lipofuscin autofluorescence in young and senescent fibroblasts. For autofluorescence quantification cells were analyzed by flow cytometry (MACSQuant[®] Analyzer 10; Miltenyi Biotec) at an excitation wavelength of 405 nm and an emission range from 425 to 475 nm. For microscopic images a confocal microscope (Ex: 405 nm, Em: 498 nm) was used. (B) Mitochondrial mass in young and senescent fibroblasts was determined by using MitoTracker Green^{FM} staining which accumulates regardless of the membrane potential in mitochondria [51]. Additionally, the abundance of different mitochondrial proteins in relation to the cell number was determined by immunoblotting. Mitochondrial superoxide was measured after MitoSOX Red incubation of cells (C). Signal intensities of MitoTracker Green^{FM} and MitoSOX were also measured by flow cytometry. * indicates statistically significant differences to young fibroblasts.

way ANOVA with Sidak's post-hoc test. Differences were considered as statistically significant, if $p < 0.05$.

3. Results

3.1. Senescent fibroblasts are marked by an increase of mitochondria and an accumulation of lipofuscin

According to our hypothesis that mitochondria contribute to the formation of lipofuscin in senescent cells we measured the lipofuscin and mitochondria content in senescent fibroblasts. An increase of lipofuscin of up to 460% in senescent fibroblasts compared to young cells was detected in our model (Fig. 1A). Interestingly, senescent fibroblasts also showed a significant increase in mitochondrial mass, measured with MitoTracker Green^{FM}, which stains mitochondria independently of their membrane potential. These data are verified by the additional determination of different mitochondrial proteins by immunoblotting (Fig. 1B). However, the increase of mitochondrial mass might not be accompanied by a stable mitochondrial functionality. Since the superoxide-/ROS-generating activity was postulated to contribute to the aging process, we assessed the formation of mitochondrial superoxide, which was significantly increased in senescent cells (Fig. 1C).

3.2. Mitochondrial function is impaired in senescent fibroblasts

Since we detected an increased mitochondrial mass and an enhanced superoxide production – indicating mitochondrial malfunction – questions on the functionality of mitochondria in senescent cells were raised. Measuring the oxygen consumption rates (OCRs) we detected a reduced mitochondrial function in senescent cells (Fig. 2A). As shown in Fig. 2B the basal OCR of senescent fibroblasts was significantly decreased in comparison to young fibroblasts (1.61 ± 0.85 vs. 3.15 ± 0.92 nmol/min/mg protein). Oligomycin treatment inhibited the ATP synthase (complex V) leading to a decreased oxygen consumption of the cells (Fig. 2A). This OCR decline from basal levels correlates with the mitochondrial ATP production which was significantly reduced in senescent fibroblasts compared to young ones (Fig. 2C). The measurement of maximum oxygen consumption after FCCP treatment revealed a reduced maximum capacity of senescent cells to consume oxygen (Fig. 2A, D). Therefore, the maximum respiration (Fig. 2D) was decreased by 40% in senescent fibroblasts compared to young fibroblasts (OCR: 3.15 ± 0.92 vs. 5.11 ± 0.53 nmol/min/mg protein). Finally, cells were treated with rotenone and antimycin A (Fig. 2A). Both substances shut down mitochondrial respira-

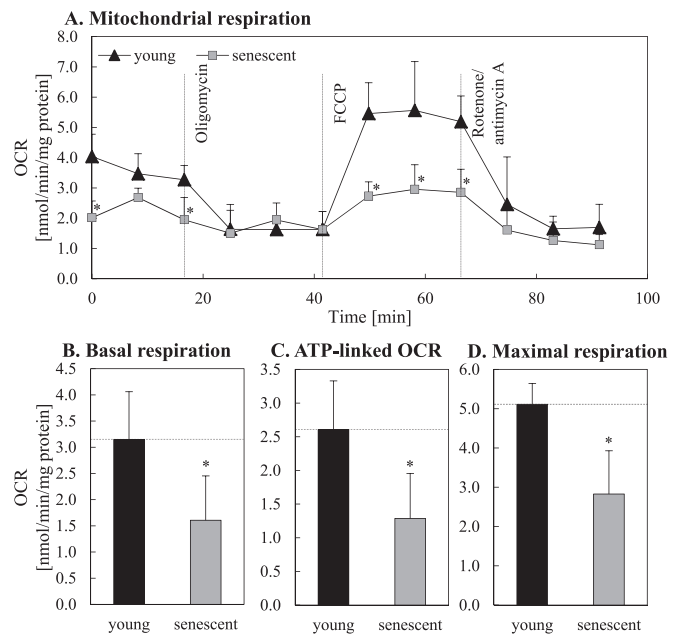


Fig. 2. Mitochondrial function in young and senescent fibroblasts. Mitochondrial function in young and senescent fibroblasts was assessed by the direct measurement of cellular oxygen consumption rates (OCRs) after the activity modulation of different electron transport chain complexes. Panel A shows the mitochondrial respiration of young and senescent cells after the successive application of oligomycin (ATP synthase inhibitor), FCCP (uncoupling agent), and a mixture of antimycin A (complex III inhibitor) and rotenone (complex I inhibitor). Based on this data the basal respiration (B), ATP production (C) as well as the maximum respiration (D) was calculated. Statistically significant differences between young and senescent fibroblasts are illustrated by *.

tion so that the remaining cellular oxygen consumption results from enzymatic activities not related to the functional mitochondrial respiratory chain.

3.3. PINK1 mediated mitophagy is reduced during aging

As we were able to show, mitochondrial function of senescent fibroblasts was reduced compared to young fibroblasts (Fig. 2) and, simultaneously, senescent fibroblasts exhibit an increased mitochondrial mass in combination with a higher mitochondrial superoxide formation (Fig. 1). Thus, we assumed a compromised mitochondrial clearance in senescent cells. The degradation of dysfunctional or

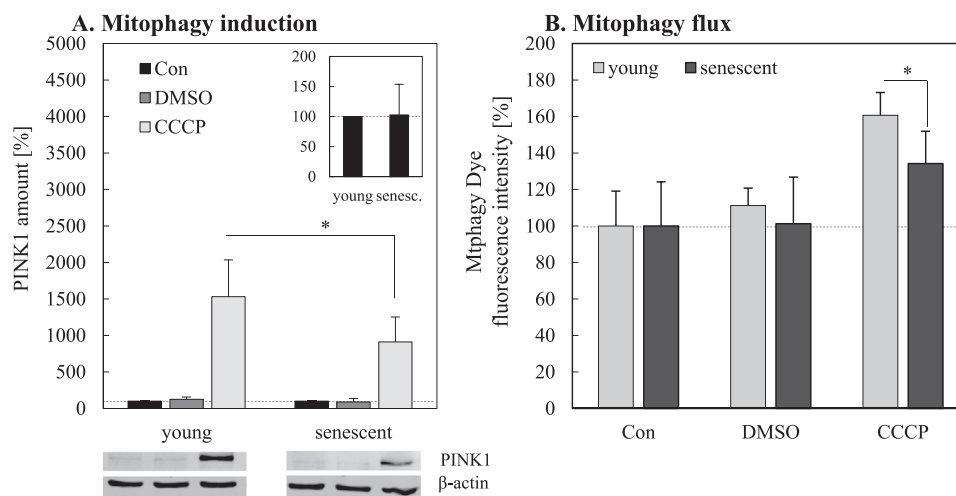


Fig. 3. Induction of mitophagy in young and senescent fibroblasts by CCCP. Twenty-four hours after treatment with the chemical uncoupling agent CCCP, PINK1 levels in young and senescent fibroblasts were assessed by immunoblotting (A). PINK1 levels in untreated controls (Con) were set to 100% (dark grey bars). PINK1 amount after CCCP treatment is shown in relation to the untreated control. DMSO serves as solvent control for CCCP. The insert shows the PINK1 levels in untreated young and senescent controls. Panel B demonstrates the uptake of mitochondria by lysosomes (mitophagy flux) after CCCP treatment in young and senescent cells. Statistical significance differences are indicated by “*”.

damaged mitochondria is mediated by their selective targeting through PINK1 and parkin followed by the removal via the mitophagy-lysosomal system. We measured the content of PINK1 in young and senescent mitochondria, which was not different (Fig. 3A, insert). However, this is not surprising since the steady state level of PINK1 is very low, due to its rapid degradation under normal conditions when no mitophagy takes place. In order to analyze the mitochondrial clearance capacity we treated young and senescent cells with CCCP which to a loss of the mitochondrial membrane potential inducing the elimination of mitochondria by mitophagy [37]. Under CCCP stimulation we were able to detect a considerable increase in cellular PINK1 content (Fig. 3A). Importantly, the PINK1 response in senescent fibroblasts was about 40% reduced compared to young fibroblasts. To evaluate, if the delivery of damaged mitochondria into lysosomes is impaired in senescent cells compared to young cells, the mitophagy flux was additionally measured by flow cytometry using a mitophagy specific dye (Mtpagy Dye) (Fig. 3B). This dye stains mitochondria, is then immobilized and changes its fluorescence intensity depending on the surrounding pH conditions. After fusion of mitochondria with lysosomes, Mtpagy Dye exhibits higher fluorescence intensity which indicates mitophagy. A significant decline of mitophagy in senescent cells after mitophagy induction with CCCP was shown.

Whereas in young cells the fluorescence intensity of Mtpagy Dye was increased to $161 \pm 12.5\%$ after CCCP treatment, senescent cells only showed a fluorescence intensity increase of $134 \pm 17.7\%$. Under starvation conditions, also known to induce mitophagy, this result was confirmed. Cultivation of young and senescent fibroblasts in the absence of FCS for 24 h similarly shows a significant change of Mtpagy Dye fluorescence intensity (data not shown).

3.4. Inhibition of mitochondrial division during PQ-induced SIPS leads to increased lipofuscin formation

Since it is known that lipofuscin accumulates in a time-dependent manner during aging [1,14,38,39] and mitophagy seems to be reduced in senescent cells (Fig. 3), it is questionable whether mitophagy contributes directly to lipofuscin formation. To investigate a possible link between these two cellular mechanisms we used an established senescence-inducing model, the PQ-mediated stress induced premature senescence (SIPS). To verify senescence induction, different markers of senescence were assessed (Fig. 4). Thus, SIPS fibroblasts are characterized by a high proportion of senescence-associated β -galactosidase positive cells (Fig. 4A). Furthermore, PQ-treated cells are

marked by decreased Ki-67 protein (Fig. 4B) and an increase in p16 as well as p21 levels (Fig. 4C). These data clearly demonstrate that PQ-treated SIPS cells have reached the senescent state. This model allows us to modulate mitochondrial turnover in an experimental senescence set-up. As demonstrated in Fig. 5A–C most of the phenotype features of senescent cells are also true for SIPS cells, however one exception is the mitochondrial mass. Incubation with Mdivi-1, an inhibitor of mitophagy, leads to an increase in mitochondrial mass. More interestingly, this increase in mitochondrial mass is accompanied by an enhanced lipofuscin formation and mitochondrial superoxide formation (Fig. 5A, C), especially when premature senescence was induced. To confirm these results we performed additional measurements of cellular ROS production and protein oxidation under these conditions (Fig. 5D, 5E). As described earlier, a malfunction of macroautophagy can lead to a slightly decreased cellular viability [40]. However, we detected no changes in the cellular viability (Fig. 5F).

These results point to an interesting fact: the blockage of mitochondrial fission leads to enhanced oxidation events which in turn result in a number of oxidative reactions and in the formation of lipofuscin. As our group has previously shown, the rate of lipofuscin formation is independent of macroautophagy [40], although formed lipofuscin is mostly located in the autophagosomal/lysosomal compartment [32]. Thus we can assume that the described general impairment of macroautophagy [25] is also true for mitophagy. Whether a fission defect is the reason for reduced mitophagy in senescent cells should be further clarified. If mitochondrial fission is involved, we would expect a larger mitochondrial network and a reduction of Fis1 as an important fission protein in senescent cells. Fig. 6 (Panels A and B) shows that these hallmarks can be observed in senescent fibroblasts.

3.5. Downregulation of Lon protease during PQ-induced SIPS is accompanied by elevated lipofuscinogenesis

Mitochondria are unique organelles possessing own proteolytic systems. It was shown that the Lon protease is able to degrade oxidatively modified proteins within mitochondria [20,22,30]. Therefore, it is interesting to investigate whether the Lon protease is altered in senescent fibroblasts. As demonstrated in Fig. 6C the protein level of Lon protease is clearly reduced in senescent fibroblasts, indicating an impaired turnover of damaged proteins inside mitochondria.

In order to examine whether the Lon protease is effectively involved in the degradation of damaged mitochondrial proteins in a senescence-

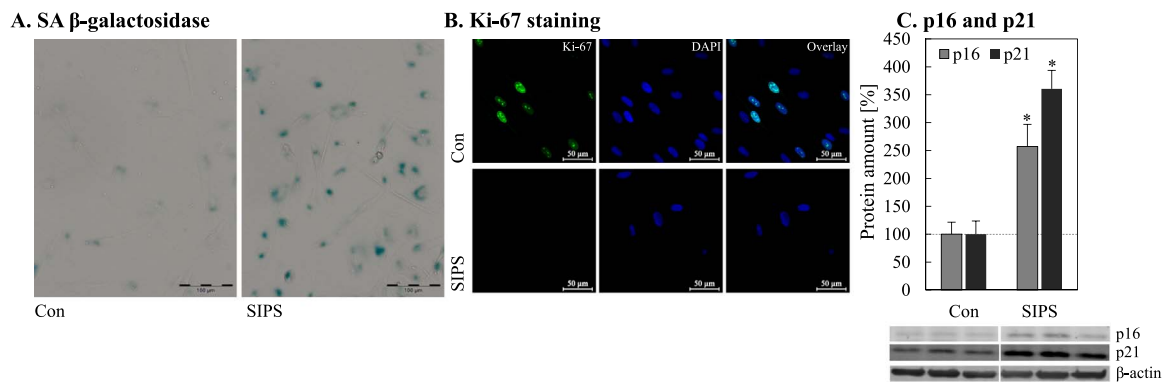


Fig. 4. Evaluation of senescence markers in SIPS cells. In order to verify the induction of premature senescence of human fibroblasts after paraquat treatment for 10 days, different senescence markers were determined: (A) senescence associated β-galactosidase activity; (B) immunostaining of the proliferation marker Ki-67, (C) protein levels of the cell cycle regulators p16 and p21. Statistical significant differences to untreated control cells are indicated by “*”.

related set-up, we used a cell line where Lon protease was down-regulated to test the effect of repeated, chronic stress on lipofuscin formation during SIPS. As shown in Fig. 7 the downregulation of Lon (Fig. 7A) resulted in an enhanced lipofuscin formation in SIPS treated cells (Fig. 7B), confirming a protective role of Lon in the prevention of lipofuscin accumulation. A combined inhibition of intra-mitochondrial Lon activity and mitophagy lead to a dramatically enhanced formation of lipofuscin (Fig. 7C).

This leads to the conclusion that both systems, intra-mitochondrial protein removal as well as the removal of damaged mitochondria as a

whole are important for the maintenance of cellular mitochondrial homeostasis.

3.6. The mitochondrial-targeted antioxidant mitoTEMPO is able to prevent SIPS-induced lipofuscin formation

Data presented here show a general role of mitochondrial proteins in cellular lipofuscin formation. However, from numerous previous studies [10,32,41–43] it seems to be clear that oxidative damage to proteins is the initial step in lipofuscin formation. Therefore, the

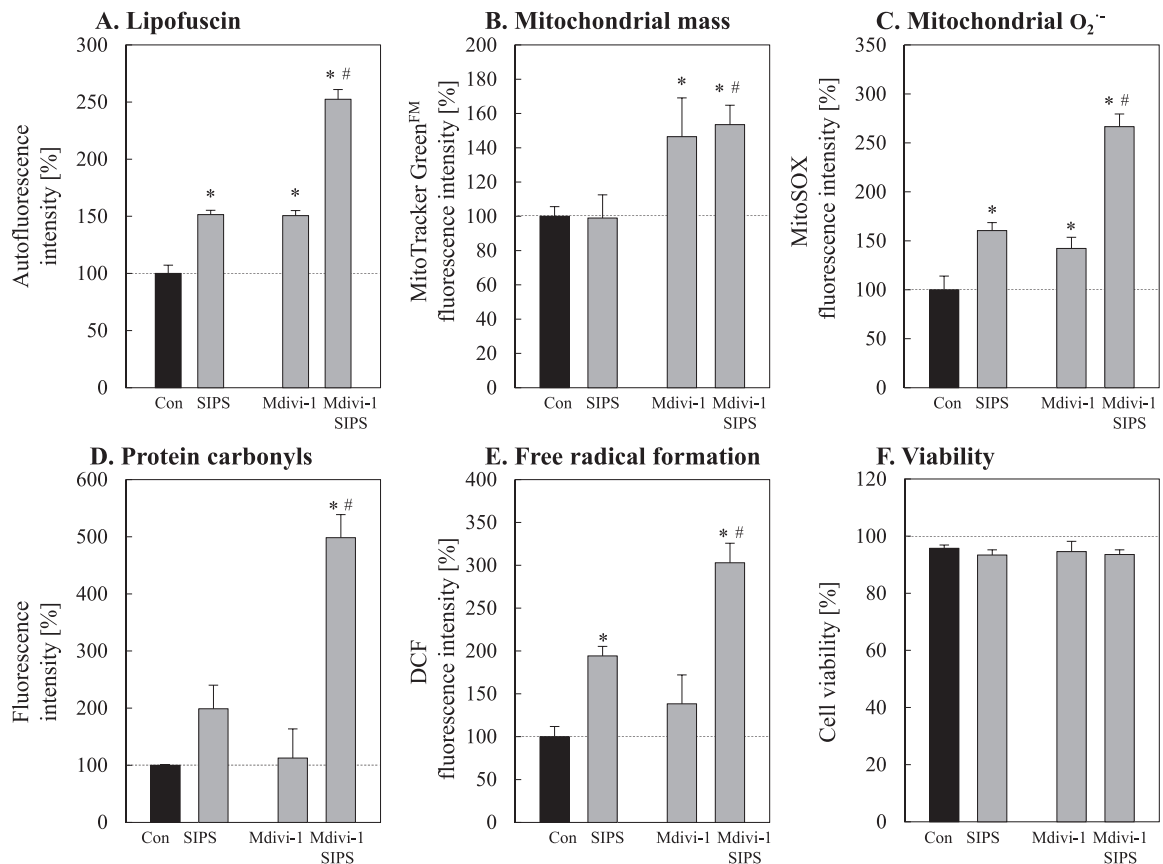


Fig. 5. Effects of reduced mitophagy on lipofuscin formation during SIPS. To investigate the influence of mitophagy inhibition on lipofuscin formation, young fibroblasts were co-treated with the mitochondrial division inhibitor 1 (Mdivi-1) during PQ-induced SIPS. Panel A shows the accumulation of lipofuscin after SIPS with or without inhibition of mitochondrial division. Lipofuscin-specific autofluorescence intensity was measured at Cell Lab Quanta™ SC MPL flow cytometer (Beckman Coulter, Krefeld, Germany) after excitation with a UV lamp (360 nm) and an emission of 525 nm. Panel B illustrates changes of the mitochondrial mass during SIPS. Mitochondrial superoxide radical formation was estimated using MitoSOX (C). In Panel D, the amounts of protein carbonyls are shown. Protein carbonyls were determined by Oxyblot. The formation of free radicals was determined by DCF fluorescence measurement (E). Panel F shows the cellular viability after SIPS treatment, assessed by propidium iodide staining. Statistically significant differences to the control are indicated by “*”, compared to respective SIPS by a “#”.

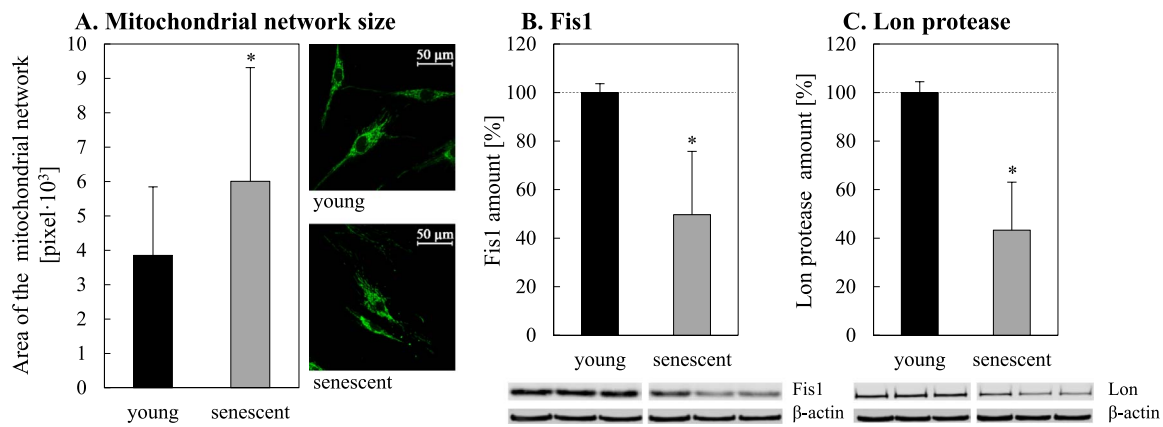


Fig. 6. Age-related changes of the mitochondrial network size and decline of Fis1 and Lon protease amounts during aging. The absolute size of the mitochondrial network was analyzed by immunofluorescence staining of the mitochondrial protein COX IV as described in the methods section (A; 50 cells were analyzed). Panels B and C show the age-related decline of Fis1 and Lon protease (Lon), respectively. Statistically significant differences to young fibroblasts are shown by ‘*’.

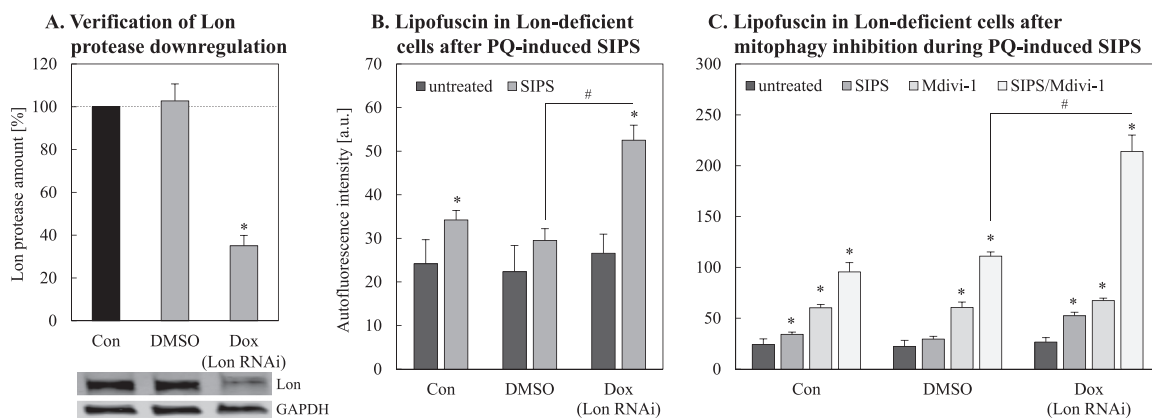


Fig. 7. Effects of Lon protease downregulation on lipofuscin formation during SIPS. HeLa cells were stably transfected with a doxycycline (Dox) inducible vector expressing a short hairpin RNA against Lon protease. Successful Lon protease downregulation was verified by immunoblot (A). Panel B represents lipofuscin accumulation after PQ-induced SIPS in Lon-deficient HeLa cells. Autofluorescence intensities were measured by Cell Lab Quanta™ SC MPL flow cytometer (Beckman Coulter, Krefeld, Germany) (Ex: 360 nm, Em: 252 nm). Panel C shows lipofuscin accumulation quantified after fission inhibition with Mdivi-1 during PQ-induced SIPS in Lon protease (Lon) deficient HeLa cells. Statistically significant differences to the corresponding control (untreated) are indicated by ‘*’, comparison to the corresponding SIPS control are marked by ‘#’.

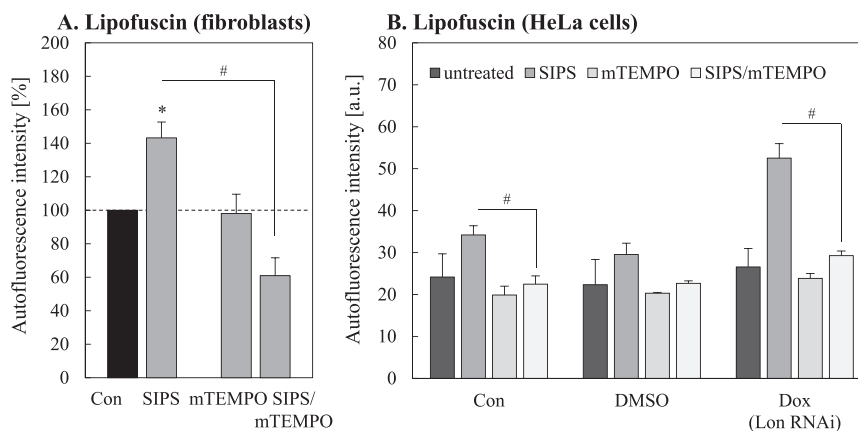


Fig. 8. Influence of mitoTEMPO on PQ-induced lipofuscin accumulation during SIPS. The effect of mitoTEMPO (mTEMPO) co-treatment with PQ during SIPS on lipofuscin accumulation in fibroblasts (A) as well as in Lon-deficient HeLa cells (B) is shown. ‘*’ marks statistically significant differences to untreated cells (Con), ‘#’ indicates statistically significant differences to the corresponding SIPS control.

question remains whether the oxidation of mitochondrial proteins is a crucial step in lipofuscin formation. In our models the reduction of mitochondrial removal via mitophagy leads to oxidative stress. Conclusively, in case this is a key step in lipofuscin formation, a protection of mitochondrial protein oxidation under conditions of reduced mitophagy should reduce lipofuscin formation. Therefore we monitored the artificial, mitochondria-targeted antioxidant

mitoTEMPO (mTEMPO) during PQ-induced SIPS (Fig. 8). Importantly, in both cellular models a significant reduction in lipofuscin formation due to this treatment was detected, indicating not only the key role of mitochondrial proteins in lipofuscin formation, but also the importance of mitochondrial protein oxidation (Fig. 8 A,B).

4. Discussion

By using a set of different cell models, we were able to demonstrate that the failure of mitochondria removal and the consecutive oxidation of mitochondrial protein are important contributors to age-related lipofuscin formation.

One reason for the functional decay during aging is the accumulation of non-degradable highly oxidized proteins forming large cellular protein aggregates. Most of these protein aggregates such as lipofuscin are located in lysosomes [40,44] suggesting a malfunction of these organelles. Cellular organelles, including mitochondria are mainly degraded by lysosomes. The lysosomal degradation of mitochondria depends on the successful separation and uncoupling of dysfunctional or damaged organelles from the mitochondrial network [37,45]. This sequestration requires fission proteins such as the mitochondrial fission 1 protein (Fis1) and the dynamin-related protein 1 (Drp1). However, this separation of damaged mitochondria from the network seems to be impaired during aging, as we detected a reduced Fis1 amount in senescent cells. The next step in the mitophagy process is then mediated by PINK1 and parkin [46]. In healthy mitochondria PINK1 is transported into the inner mitochondrial membrane where it is cleaved by the rhomboid protease presenilin-associated rhomboid-like protein (PARL) [47]. Malfunctioned mitochondria are marked by the stabilization of PINK1 on the outer mitochondrial membrane; this accumulation of PINK1 was reduced in senescent cells. PINK1 recruits the cytosolic protein parkin, which acts as E3-ubiquitin ligase and triggers the ubiquitination of several mitochondrial outer membrane proteins. Ubiquitination is succeeded by the recruitment of p62 and further proteins which finally result in the engulfment of impaired mitochondria by the autophagosome. Fusion of the mitochondria-filled autophagosome with a lysosome may provide degrading enzymes such as cathepsins for the actual degradation. However, it is hypothesized that the failure of this degradation in the lysosome is causative for lipofuscinogenesis. To prove this theory we investigated the influence of mitophagy inhibition on lipofuscin formation by using Mdivi-1 during PQ-induced SIPS. Mdivi-1 is a selective chemical inhibitor of Drp1 resulting in an inhibition of the mitochondrial fission [48] thereby blocking mitophagy [49] resulting in an increased cellular mitochondrial mass. Interestingly, in senescent cells as well as the SIPS models used in this study, an increased mitochondrial mass is accompanied by an enhanced lipofuscin formation, indicating an association. Since the increase of mitochondrial mass in senescent cells was accompanied by a decline in mitochondrial function, we can state that the accumulation of dysfunctional mitochondria occurs during aging. Furthermore, it was shown that the accumulation of dysfunctional mitochondria results in elevated ROS formation [23,50] and is therefore an explanation for the observation of higher lipofuscin amounts in our cellular models.

Additionally, we previously demonstrated that lipofuscin formation might take place outside the lysosomal compartment and is indeed independent of the macroautophagic process [40]. Because mitophagy and also autophagy in general decrease during aging, but the formation of lipofuscin increases simultaneously, autophagic processes alone cannot be responsible for lipofuscinogenesis. Nevertheless, our data demonstrate a clear contribution of mitochondrial protein degradation mechanisms to lipofuscin formation.

In the present study we were able to experimentally demonstrate for the first time the crucial involvement of oxidized mitochondrial proteins in the formation of lipofuscin. Thus we postulate that the initial steps of cross-linking and lipofuscin formation from mitochondrial proteins may also take place outside the lysosomal compartment. These findings are in agreement with our previous work.

Acknowledgments

We kindly thank Prof. Annette Schürmann for providing the XF-24-

3 extracellular flux analyzer device for the measurement of the oxygen consumption rates. This work was supported by the DFG (German Research Foundation). The authors declare no conflict of interest.

References

- [1] T. von Zglinicki, E. Nilsson, W.D. Docke, U.T. Brunk, Lipofuscin accumulation and ageing of fibroblasts, *Gerontology* 41 (Suppl. 2) (1995) 95–108.
- [2] A. Terman, U.T. Brunk, The aging myocardium: roles of mitochondrial damage and lysosomal degradation, *Heart Lung Circ.* 14 (2005) 107–114.
- [3] N. Sitte, M. Huber, T. Grune, A. Ladhoff, W.D. Doecke, T. Von Zglinicki, K.J. Davies, Proteasome inhibition by lipofuscin/ceoid during postmitotic aging of fibroblasts, *FASEB J.: Off. Publ. Fed. Am. Soc. Exp. Biol.* 14 (2000) 1490–1498.
- [4] E. Couve, R. Osorio, O. Schmachtenberg, Mitochondrial autophagy and lipofuscin accumulation in aging odontoblasts, *J. Dent. Res.* 91 (2012) 696–701.
- [5] A. Höhn, T. Jung, S. Grimm, B. Catalgol, D. Weber, T. Grune, Lipofuscin inhibits the proteasome by binding to surface motifs, *Free Radic. Biol. Med.* 50 (2011) 585–591.
- [6] E. Sugano, H. Tomita, S. Ishiguro, H. Isago, M. Tamai, Nitric oxide-induced accumulation of lipofuscin-like materials is caused by inhibition of cathepsin S, *Curr. Eye Res.* 31 (2006) 607–616.
- [7] S.R. Powell, P. Wang, A. Divald, S. Teichberg, V. Haridas, T.W. McCloskey, K.J. Davies, H. Katzeff, Aggregates of oxidized proteins (lipofuscin) induce apoptosis through proteasome inhibition and dysregulation of proapoptotic proteins, *Free Radic. Biol. Med.* 38 (2005) 1093–1101.
- [8] Y. Stroikin, H. Dalen, S. Loof, A. Terman, Inhibition of autophagy with 3-methyladenine results in impaired turnover of lysosomes and accumulation of lipofuscin-like material, *Eur. J. Cell Biol.* 83 (2004) 583–590.
- [9] A. Terman, S. Sandberg, Proteasome inhibition enhances lipofuscin formation, *Ann. N. Y. Acad. Sci.* 973 (2002) 309–312.
- [10] A. Höhn, T. Jung, S. Grimm, T. Grune, Lipofuscin-bound iron is a major intracellular source of oxidants: role in senescent cells, *Free Radic. Biol. Med.* 48 (2010) 1100–1108.
- [11] C.Q. Mountjoy, J.H. Dowson, C. Harrington, M.R. Cairns, H. Wilton-Cox, Characteristics of neuronal lipofuscin in the superior temporal gyrus in Alzheimer's disease do not differ from non-diseased controls: a comparison with disease-related changes in the superior frontal gyrus, *Acta Neuropathol.* 109 (2005) 490–496.
- [12] N. Ulfsg, Altered lipofuscin pigmentation in the basal nucleus (Meynert) in Parkinson's disease, *Neurosci. Res.* 6 (1989) 456–462.
- [13] A. Gheorghie, L. Mahdi, O. Musat, Age-related macular degeneration, *Rom. J. Ophthalmol.* 59 (2015) 74–77.
- [14] U.T. Brunk, A. Terman, The mitochondrial-lysosomal axis theory of aging: accumulation of damaged mitochondria as a result of imperfect autophagocytosis, *Eur. J. Biochem* 269 (2002) 1996–2002.
- [15] J. Ezaki, L.S. Wolfe, E. Kominami, Defect of proteolysis of mitochondrial ATP synthase subunit C in neuronal ceroid lipofuscinosis, *Gerontology* 41 (Suppl. 2) (1995) 259–269.
- [16] L.D. Gauthier, J.L. Greenstein, B. O'Rourke, R.L. Winslow, An integrated mitochondrial ROS production and scavenging model: implications for heart failure, *Biophys. J.* 105 (2013) 2832–2842.
- [17] M.P. Murphy, How mitochondria produce reactive oxygen species, *Biochem. J.* 417 (2009) 1–13.
- [18] M. Lagouge, N.G. Larsson, The role of mitochondrial DNA mutations and free radicals in disease and ageing, *J. Intern. Med.* 273 (2013) 529–543.
- [19] J. Blasiak, G. Hoser, J. Bialkowska-Warzecha, E. Pawlowska, T. Skorski, Reactive oxygen species and mitochondrial DNA damage and repair in BCR-ABL1 cells resistant to Imatinib, *BioResearch Open Access* 4 (2015) 334–342.
- [20] D.A. Bota, K.J. Davies, Lon protease preferentially degrades oxidized mitochondrial acanovite by an ATP-stimulated mechanism, *Nat. Cell Biol.* 4 (2002) 674–680.
- [21] K. Davies, Protective role of the mitochondrial Lon protease in homeostasis, oxidative stress-adaptation, disease, and aging, *Faseb J.* 28 (2014).
- [22] J.K. Ngo, K.J. Davies, Importance of the Lon protease in mitochondrial maintenance and the significance of declining lon in aging, *Ann. N. Y. Acad. Sci.* 1119 (2007) 78–87.
- [23] M.A. Bin-Umer, J.E. McLaughlin, M.S. Butterly, S. McCormick, N.E. Tumer, Elimination of damaged mitochondria through mitophagy reduces mitochondrial oxidative stress and increases tolerance to trichothecenes, *Proc. Natl. Acad. Sci. USA* 111 (2014) 11798–11803.
- [24] H. Wei, L. Liu, Q. Chen, Selective removal of mitochondria via mitophagy: distinct pathways for different mitochondrial stresses, *Biochim. Biophys. Acta* 1853 (2015) 2784–2790.
- [25] C. Ott, J. König, A. Höhn, T. Jung, T. Grune, Reduced autophagy leads to an impaired ferritin turnover in senescent fibroblasts, *Free Radic. Biol. Med.* (2016).
- [26] C. Ott, J. König, A. Höhn, T. Jung, T. Grune, Macroautophagy is impaired in old murine brain tissue as well as in senescent human fibroblasts, *Redox Biol.* (2016) (In press).
- [27] L. Chen, A.J. Winger, A.A. Knowlton, Mitochondrial dynamic changes in health and genetic diseases, *Mol. Biol. Rep.* 41 (2014) 7053–7062.
- [28] K. Atkins, A. Dasgupta, K.H. Chen, J. Mewburn, S.L. Archer, The role of Drp1 adaptor proteins Mid49 and Mid51 in mitochondrial fission: implications for human disease, *Clin. Sci.* 130 (2016) 1861–1874.
- [29] J. König, F. Besoke, W. Stuetz, A. Malarski, G. Jahreis, T. Grune, A. Hohn, Quantification of age-related changes of alpha-tocopherol in lysosomal membranes in murine tissues and human fibroblasts, *BioFactors* 42 (2016) 307–315.

- [30] A. Bayot, M. Gareil, L. Chavatte, M.P. Hamon, C. L'Hermitte-Stead, F. Beaumatin, M. Priault, P. Rustin, A. Lombes, B. Friguet, A.L. Bulteau, Effect of Lon protease knockdown on mitochondrial function in HeLa cells, *Biochimie* 100 (2014) 38–47.
- [31] B. Lu, S. Yadav, P.G. Shah, T. Liu, B. Tian, S. Puksza, N. Villaluna, E. Kutejova, C.S. Newlon, J.H. Santos, C.K. Suzuki, Roles for the human ATP-dependent Lon protease in mitochondrial DNA maintenance, *J. Biol. Chem.* 282 (2007) 17363–17374.
- [32] T. Jung, A. Höhn, B. Catalgol, T. Grune, Age-related differences in oxidative protein-damage in young and senescent fibroblasts, *Arch. Biochem. Biophys.* 483 (2009) 127–135.
- [33] T. Jung, A. Höhn, T. Grune, Lipofuscin: detection and quantification by microscopic techniques, *Methods Mol. Biol.* 594 (2010) 173–193.
- [34] O.H. Lowry, N.J. Rosebrough, A.L. Farr, R.J. Randall, Protein measurement with the Folin phenol reagent, *J. Biol. Chem.* 193 (1951) 265–275.
- [35] I. Dalle-Donne, R. Rossi, D. Giustarini, A. Milzani, R. Colombo, Protein carbonyl groups as biomarkers of oxidative stress, *Clin. Chim. Acta* 329 (2003) 23–38.
- [36] R.L. Levine, J.A. Williams, E.R. Stadtman, E. Shacter, Carbonyl assays for determination of oxidatively modified proteins, *Methods Enzym.* 233 (1994) 346–357.
- [37] G. Twig, A. Elorza, A.J. Molina, H. Mohamed, J.D. Wikstrom, G. Walzer, L. Stiles, S.E. Haigh, S. Katz, G. Las, J. Alroy, M. Wu, B.F. Py, J. Yuan, J.T. Deeney, B.E. Corkey, O.S. Shirihai, Fission and selective fusion govern mitochondrial segregation and elimination by autophagy, *EMBO J.* 27 (2008) 433–446.
- [38] A. Terman, T. Kurz, M. Navratil, E.A. Arriaga, U.T. Brunk, Mitochondrial turnover and aging of long-lived postmitotic cells: the mitochondrial-lysosomal axis theory of aging, *Antioxid. Redox Signal* 12 (2010) 503–535.
- [39] N. Sitte, K. Merker, T. Grune, T. von Zglinicki, Lipofuscin accumulation in proliferating fibroblasts in vitro: an indicator of oxidative stress, *Exp. Gerontol.* 36 (2001) 475–486.
- [40] A. Höhn, A. Sittig, T. Jung, S. Grimm, T. Grune, Lipofuscin is formed independently of macroautophagy and lysosomal activity in stress-induced prematurely senescent human fibroblasts, *Free Radic. Biol. Med.* 53 (2012) 1760–1769.
- [41] T. Grune, K. Merker, T. Jung, N. Sitte, K.J. Davies, Protein oxidation and degradation during postmitotic senescence, *Free Radic. Biol. Med.* 39 (2005) 1208–1215.
- [42] A. Höhn, J. König, T. Grune, Protein oxidation in aging and the removal of oxidized proteins, *J. Proteom.* 92 (2013) 132–159.
- [43] S. Reeg, T. Grune, Protein oxidation in aging: does it play a role in aging progression?, *Antioxid. Redox Signal* 23 (2015) 239–255.
- [44] A. Soleiman, A. Lukschal, S. Hacker, K. Aumayr, K. Hoetzenecker, M. Lichtenauer, B. Moser, E. Untermayr, R. Horvat, H.J. Ankersmit, Myocardial lipofuscin-laden lysosomes contain the apoptosis marker caspase-cleaved cytokeratin-18, *Eur. J. Clin. Invest* 38 (2008) 708–712.
- [45] K. Mao, D.J. Klionsky, Participation of mitochondrial fission during mitophagy, *Cell Cycle* 12 (2013) 3131–3132.
- [46] S.M. Jin, R.J. Youle, PINK1- and Parkin-mediated mitophagy at a glance, *J. Cell Sci.* 125 (2012) 795–799.
- [47] S.M. Jin, M. Lazarou, C. Wang, L.A. Kane, D.P. Narendra, R.J. Youle, Mitochondrial membrane potential regulates PINK1 import and proteolytic destabilization by PARL, *J. Cell Biol.* 191 (2010) 933–942.
- [48] A. Cassidy-Stone, J.E. Chipuk, E. Ingerman, C. Song, C. Yoo, T. Kuwana, M.J. Kurth, J.T. Shaw, J.E. Hinshaw, D.R. Green, J. Nunnari, Chemical inhibition of the mitochondrial division dynamin reveals its role in Bax/Bak-dependent mitochondrial outer membrane permeabilization, *Dev. Cell* 14 (2008) 193–204.
- [49] S. Givvimani, C. Munjal, N. Tyagi, U. Sen, N. Metreveli, S.C. Tyagi, Mitochondrial division/mitophagy inhibitor (Mdivi) ameliorates pressure overload induced heart failure, *PLoS One* 7 (2012) e32388.
- [50] A. Hoshino, Y. Mita, Y. Okawa, M. Ariyoshi, E. Iwai-Kanai, T. Ueyama, K. Ikeda, T. Ogata, S. Matoba, Cytosolic p53 inhibits Parkin-mediated mitophagy and promotes mitochondrial dysfunction in the mouse heart, *Nat. Commun.* 4 (2013) 2308.
- [51] W. Pendergrass, N. Wolf, M. Poot, Efficacy of MitoTracker green (TM) and CMXRosamine to measure changes in mitochondrial membrane potentials in living cells and tissues, *Cytom. A* 61a (2004) 162–169.